Altered sensitivities to morphine and cocaine in scaffold protein tamalin knockout mice

Masaaki Ogawa*†, Tsuyoshi Miyakawa‡§, Kenji Nakamura¶, Jun Kitano†∥, Kenryo Furushima**, Hiroshi Kiyonari**, Rika Nakayama**, Kazuki Nakao**, Koki Moriyoshi††, and Shigetada Nakanishi*†,††‡‡

*Department of Systems Biology, Osaka Bioscience Institute, Suita, Osaka 565-0874, Japan; †Department of Biological Sciences and ‡Horizontal Medical Research Organization, Faculty of Medicine, and ††Department of Molecular and System Biology, Graduate School of Biostudies, Kyoto University, Sakyo-ku, Kyoto 606-8501, Japan; ¶Mouse Genome Technology Laboratory, Mitsubishi Kagaku Institute of Life Sciences, Machida, Tokyo 194-8511, Japan; and **Laboratory for Animal Resources and Genetic Engineering, RIKEN Center for Developmental Biology, Chuo-ku, Kobe, Hyogo 650-0046, Japan

Tamalin is a scaffold protein that interacts with metabotropic glutamate receptors and the kinase-deficient neurotrophin TrkCT1 receptor and forms a protein complex with multiple protein-trafficking and intracellular signaling molecules. In culture, tamalin promotes intracellular trafficking of group 1 metabotropic glutamate receptors through its interaction with guanine nucleotide exchange factor cytohesins and causes actin reorganization and membrane ruffling via the TrkCT1/cytohesin-2 signaling mechanism. However, how tamalin serves its physiological function *in vivo* has remained elusive. In this study, we generated tamalin knockout (Tam⁻/⁻ KO) mice and investigated behavioral alterations resulting from their deficiency in functional tamalin. Targeted deletion of functional tamalin altered neither the overall brain architecture nor the general behavior of the mice under ordinary conditions. However, Tam⁻/⁻ KO mice showed a decrease in sensitivity to acute morphine-induced hyperlocomotion and morphine analgesic effects in the hot-plate test. Furthermore, tamalin deficiency impaired the ability of the animals to show conditioned place preference after repeated morphine administration and to display locomotor sensitization by chronic cocaine treatment. Upon *in vivo* microdialysis analysis of the nucleus accumbens, Tam⁻/⁻ KO and wild-type mice showed no genotypic differences in their response patterns of extracellular dopamine and glutamate before or after morphine administration. These results demonstrate that the tamalin scaffold protein plays a unique role in both acute and adaptive behavioral responses to morphine and cocaine and could regulate common neural substrates implicated in drugs of abuse.

addiction | analgesia | metabotropic glutamate receptor | PDZ domain | protein complex

Multimolecular protein assembly involving postsynaptic receptors is important for spatiotemporal regulation of receptor localization, signal transduction, and synaptic plasticity in neuronal cells (1, 2). Scaffold proteins that contain multiple domains for protein–protein interaction are required for the efficient and selective molecular assembly of protein complexes (3, 4). Tamalin (also called GRP1-associated scaffold protein) is a scaffold protein composed of multiple protein-interacting domains, including a PSD-95/discs-large/ZO-1 (PDZ) domain, a leucine zipper region, and a carboxyl-terminal PDZ binding motif (5, 6). Tamalin forms a protein complex with group 1/2 metabotropic glutamate receptors (mGluRs) and guanine nucleotide exchange factor cytohesins and promotes intracellular trafficking and cell-surface expression of group 1 mGluRs in transfected COS-7 cells and cultured hippocampal neurons (5, 6). Tamalin also binds to other scaffold proteins such as PSD-95, Mint2, and CASK, all of which are involved in postsynaptic organization and protein trafficking (7). Tamalin is phosphorylated at tyrosines of its immunoreceptor tyrosine-based activation motif sequence by the Src family kinases and, in turn, activates Syk kinase (8). A recent study further revealed that

tamalin links a kinase-deficient neurotrophin receptor, TrkCT1, to the cytohesin-2/ADP-ribosylation factor 6 (ARF6) signaling in a neurotrophin-3-dependent manner and causes membrane ruffling and actin reorganization (9). Tamalin mRNA expression overlaps with that of group 1 mGluR and TrkCT1 mRNAs and is developmentally up-regulated during the postnatal period in the telencephalic region of the brain (5, 7, 9). However, the physiological role of tamalin in neuronal development, synaptic plasticity, and various behaviors remains elusive.

In the present study, we established tamalin knockout (Tam⁻/⁻ KO) mice and investigated developmental and behavioral alterations resulting from targeted deletion of tamalin. Tam⁻/⁻ KO mice developed normally and showed no abnormal behaviors under ordinary conditions. However, tamalin deficiency resulted in a marked reduction in sensitivity to acute morphine responses and impaired adaptive responses to morphine and cocaine. The tamalin scaffold protein thus plays a pivotal role in the responsiveness to actions of both morphine and cocaine.

Results

Generation of Tam⁻/⁻ KO Mice. The PDZ domain and the leucine zipper region of tamalin bind to the carboxyl-terminal region of group 1 mGluRs and the coiled-coil region of cytohesins, respectively (5). To circumvent possible lethality of conventional Tam⁻/⁻ KO mice, we decided to generate not only conventional KO mice with tamalin deficiency in their whole body, but also conditional KO mice lacking tamalin restrictedly in the brain. A targeting vector was constructed in which a neomycin-resistance gene (*Neo*) and exons 5–7 encoding the carboxyl-terminal half of the PDZ domain and the entire leucine zipper region of tamalin were flanked by three *loxP* sites (Fig. 1*A*). Under this design, the excision of both *Neo* and exons 5–7 by Cre recombinase generates conventional KO mice, whereas the excision of *Neo* alone provides a transgenic (floxed) line from which conditional KO mice can be produced by crossing with brain-specific *Cre* transgenic mice (10). We first generated a mouse line in which the *Neo* and three *loxP* sites were inserted in the tamalin gene. We succeeded in generating the two types of mutated mice by crossing them with *EIIa* promoter-driven *Cre* (*EIIa-Cre*) trans-
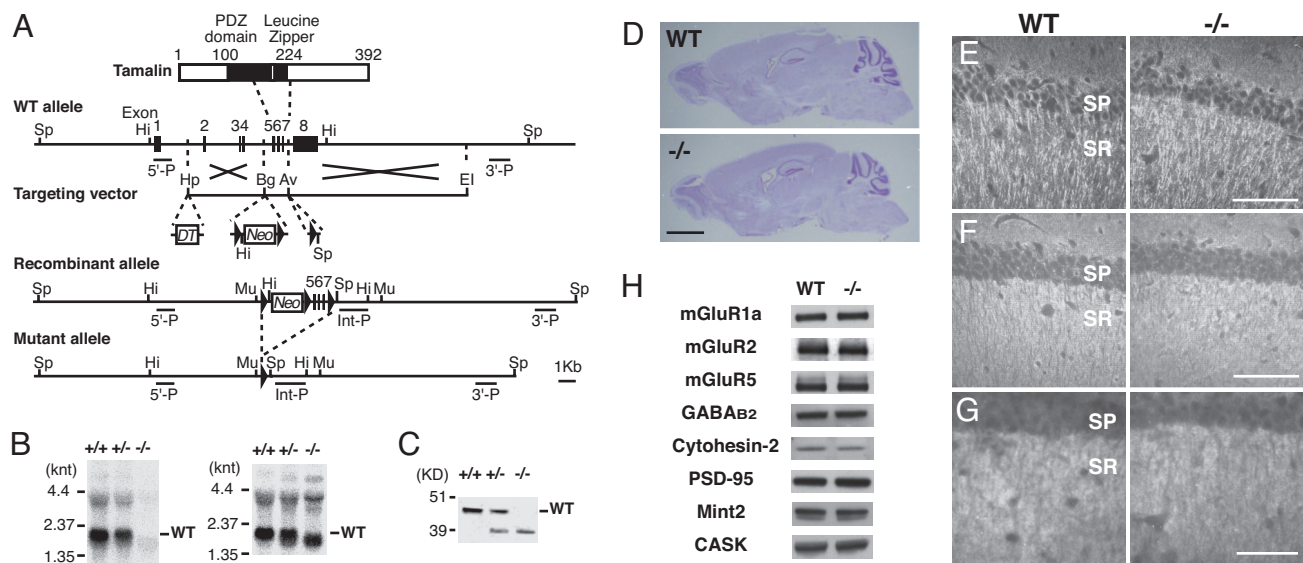
NEUROSCIENCE

Fig. 1. Generation and characterization of Tam$^{-/-}$ KO mice. (*A*) Strategy for generation of Tam$^{-/-}$ KO mice. The WT allele of the tamalin gene (second diagram) is shown along with the structure of the tamalin protein (first diagram) as a reference. In the targeting vector (third diagram), exons 5–7 encoding the middle part of tamalin and *Neo* were flanked by three *loxP* sites, and a diphtheria toxin-A gene (*DT*) was attached to the 5′ side of the targeting gene for negative selection. HpaI (Hp), BglII (Bg), AvrII (Av), and EcoRI (EI) restriction sites were used for vector construction. Diagnostic HindIII (Hi) and SpeI (Sp) restriction sites and a 5′ probe (5′-P) and a 3′ probe (3′-P) were used to identify the correctly targeted recombinant allele in ES clones (fourth diagram). The resultant mouse line containing the recombinant allele was crossed with *EIIa-Cre* transgenic mice to remove exons 5–7 and the *Neo* gene (bottom diagram). Removal of these DNA sequences was confirmed with an internal probe (Int-P) after MunI (Mu) digestion. (*B*) Northern blot analysis of tamalin mRNA expression. cDNAs encoding exons 5–7 (*Left*) and exons 1–7 (*Right*) were used to probe total RNA isolated from adult whole brains; knt, kilonucleotides. (*C*) Immunoblot analysis of tamalin. Total homogenates of the adult whole brain were immunoblotted with anti-tamalin antibody; KD, kilodaltons. (*D*) Nissl staining of parasagittal sections of adult whole brains. (*E–G*) Immunofluorescence analysis of the hippocampal CA1 region with antibodies against MAP2 (*E*), synaptophysin (*F*), and mGluR5 (*G*). SP, pyramidal cell layer; SR, stratum radiatum. (*H*) Immunoblot analysis of homogenates prepared from the striatum. In *D–H*, no difference was observed between the two genotypes. (Scale bars: *D*, 2 mm; *E* and *F*, 70 μm; *G*, 40 μm.)

genic mice on a C57BL/6 genetic background (10, 11). We found that the conventional homozygous Tam$^{-/-}$ KO mice were viable and fertile with a normal Mendelian ratio of genotypes in the offspring [69:152:71 for wild-type (WT)/heterozygous/homozygous mutant mice]. We generated two independent lines of conventional Tam$^{-/-}$ KO mice and confirmed no phenotypic difference between them. Therefore, we used one line of these conventional KO mice in all subsequent experiments. Northern blot analysis with cDNAs of exons 5–7 used as a probe showed the lack of tamalin mRNA in the brain of Tam$^{-/-}$ KO mice (Fig. 1*B Left*). However, a probe covering the exon 1–7 sequence displayed expression of the short-length tamalin mRNA (Fig. 1*B Right*). Reverse transcriptase–PCR analysis disclosed that this mRNA was devoid of the exon 5–7 sequence and that the exon 4 sequence was directly linked to the exon 8 sequence. Because the amino acid sequence encoded by exon 4 was connected in-frame with that encoded by exon 8, a low level of the tamalin protein lacking the exon 5–7-encoding 76-aa sequence was also detected in brain lysates (Fig. 1*C*). However, this aberrant tamalin with the deletion is defective, because the carboxyl-terminal half of the PDZ domain and the leucine zipper region are essential for binding to the PDZ-binding motif and cyto-hesins, respectively (3, 5, 6).

Nissl staining and immunostaining for the dendritic marker MAP2 and the presynaptic marker synaptophysin showed no overall alteration in the brain architecture, nor any morphological abnormality of neuronal cells (Fig. 1 *D–F*). The expression levels of tamalin-interacting proteins, including mGluR1a, mGluR2, mGluR5, GABA$_{B2}$ receptor, cytohesin-2, PSD-95, Mint2, and CASK (5, 7), remained unchanged in striatum homogenates from Tam$^{-/-}$ KO mice as compared with their levels in WT mice (Fig. 1*H*). Also, no obvious change in the

distribution pattern of mGluR5 immunoreactivity was noted in the hippocampus (Fig. 1*G*).

General Characteristics of Tam$^{-/-}$ KO Mice. To address whether tamalin deficiency affects any physical or behavioral characteristics, we subjected Tam$^{-/-}$ KO mice and their WT littermates to a comprehensive battery of physical and behavioral tests (12, 13). Tam$^{-/-}$ KO mice were healthy and showed no alteration in physical characteristics (body weight, appearance of fur and whiskers, and rectal temperature), in behavior involving sensory/motor functions (wire hang, grip strength, sensory-motor reflex, prepulse inhibition, and rotarod test), or in emotional behaviors (light/dark transition, elevated plus maze, social interaction, and forced swim tests).

Acute Responses to Morphine in Tam$^{-/-}$ KO Mice. The distribution of tamalin mRNA, and that of mGluR5 mRNA, correlates well in the striatum, nucleus accumbens (NAc), cerebral cortex, and hippocampus, which serve as critical neural substrates for actions of drugs of abuse (5, 14–18). Furthermore, group 1 mGluRs are important for both acute response to addictive drugs and neural plasticity in drug addiction (17, 18). So we addressed whether the tamalin deficiency would affect behavioral responses to acute morphine administration (Fig. 2). When total distance traveled in an open field for 1 h was counted, there was no difference in the locomotor activity in the new environment between WT and Tam$^{-/-}$ KO mice [WT, 9,373.6 ± 377.2 cm; KO, 8,813.9 ± 325.2 cm; $P = 0.262$; $n = 33$ (WT) and 38 (KO)]. These mice were again habituated to the open field for 1 h on the fourth day after the first test, and the locomotor activity was then counted every 5 min for 2 h after the s.c. administration of morphine. Both WT and Tam$^{-/-}$ KO mice showed a progressive increase in locomotor activity after the injection of morphine (for min, 2.5 mg/kg,
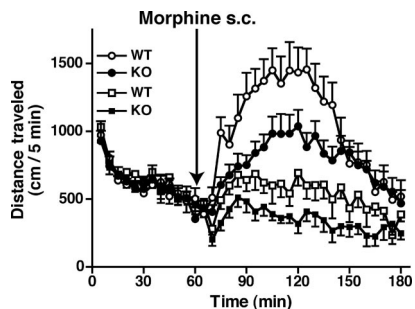
Fig. 2. Acute effect of morphine administration on locomotor activity. After 1-h habituation, morphine (2.5 mg/kg or 5 mg/kg) was s.c. administered to WT and Tam$^{-/-}$ KO mice, and the distance traveled was counted every 5 min for 120 min; squares, 2.5 mg/kg morphine; circles, 5 mg/kg morphine.

$P < 0.0001$; 5 mg/kg, $P < 0.0001$), but the morphine-induced hyperlocomotion was significantly reduced in Tam$^{-/-}$ KO mice compared with WT mice (Fig. 2). When the total distance traveled was counted during the acute phase (the first 60 min) of the morphine responses (Fig. 2), Tam$^{-/-}$ KO mice showed significantly less morphine-induced hyperlocomotion than WT mice at 2.5 mg/kg morphine [WT, 6,928.3 ± 705.9 cm; KO, 4,650.7 ± 550.7 cm; $P = 0.018$; $n = 9$ (WT) and 11 (KO)] and 5 mg/kg morphine [WT, 13,513.8 ± 1,463.2 cm; KO, 9,322.6 ± 809.9 cm; $P = 0.017$; $n = 12$ (WT) and 13 (KO)], but not at 10 mg/kg morphine [WT, 20,836.3 ± 3,432.8 cm; KO, 23,107.0 ± 3194.0 cm; $P = 0.637$; $n = 6$ (WT) and 7 (KO)]. The results indicate that tamalin deficiency reduces the sensitivity to morphine during the acute phase of the morphine-induced hyperlocomotion.

We next tested antinociceptive responses to morphine by conducting hot-plate and tail-flick tests (Fig. 3). Tam$^{-/-}$ KO mice exhibited normal nociceptive thresholds in both the hot-plate test (52°C, $P = 0.659$; 55°C, $P = 0.861$, $n = 9$–11) (Fig. 3A) and the tail-flick test [$P = 0.659$, $n = 11$ (WT) and 9 (KO)] (Fig. 3B). When the acute analgesic effect was examined in the hot-plate test every 15 min after administration of 10 mg/kg morphine, Tam$^{-/-}$ KO mice showed a significant decrease in their analgesic response to morphine during the first 45 min [for genotype, $P = 0.049$; interaction genotype × min, $P = 0.142$, $n = 10$ (WT), $n = 11$ (KO)] (Fig. 3C). However, the duration of the morphine analgesic effect (about 90 min) was not changed by the tamalin deficiency (Fig. 3C). When the dose–response relationship of the acute morphine analgesic effect was examined 30 min after morphine administration, a significant difference was observed at 10 mg/kg morphine [$P = 0.015$, $n = 6$ (WT) and 7 (KO)] but not at 20 mg/kg morphine [$P = 0.308$, $n = 8$ (WT) and 9 (KO)] (Fig. 3D), indicating again the significant reduction in the sensitivity to morphine in the tamalin-deficient mice. In contrast to the results from the hot-plate test, no difference in the sensitivity to morphine in the tail-flick test was observed between the two genotypes [2.5 mg/kg, $P = 0.423$; 5 mg/kg, $P = 0.315$, $n = 6$–9] (Fig. 3E). In general, it has been accepted that the hot-plate response involves supraspinal analgesia, whereas the tail-flick response mainly occurs at the level of the spinal cord (19). Therefore, the results obtained for two different behavioral paradigms (locomotor activity and hot-plate analgesic response) indicate that tamalin plays an important role in acute morphine-induced responses at the supraspinal level.

In Tam$^{-/-}$ KO mice, neither morphine antinociceptive tolerance nor morphine withdrawal effects (20) were altered. When the morphine antinociceptive effects were examined by the hot-plate test after daily administration of 10 mg/kg morphine, antinociceptive tolerance developed in both WT and Tam$^{-/-}$ KO mice, but no genotypic difference was noted [for genotype,
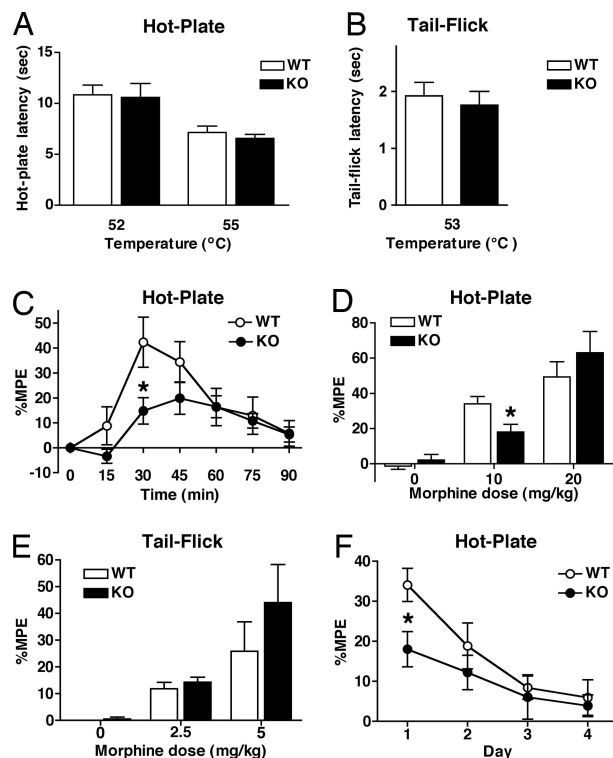
Fig. 3. Analgesic responses to morphine in the hot-plate and tail-flick tests. (*A* and *B*) Nociceptive thresholds were tested by measuring latencies of analgesic responses in the hot-plate test (*A*) and in the tail-flick test (*B*). (*C*) Analgesic responses to morphine were examined in the hot-plate test 15 min after s.c. injection of 10 mg/kg morphine [∗, $P = 0.022$, $n = 10$ (WT) and 11 (KO)]. %MPE, percentage of maximal possible effect. (*D* and *E*) Dose–responses of analgesic effects of morphine in the hot-plate test (*D*) and the tail-flick test (*E*). Analgesic responses were examined 30 min after s.c. injection of the indicated doses of morphine (∗, $P = 0.015$, $n = 6$–9). (*F*) Development of morphine analgesic tolerance was examined once a day 30 min after administration of 10 mg/kg morphine [∗, $P = 0.015$, $n = 7$ (WT) and 6 (KO)].

$P = 0.155$; for day, $P < 0.0001$; interaction genotype × day, $P = 0.196$, $n = 7$ (WT) and 6 (KO)] (Fig. 3F). To examine morphine-induced physical dependence, mice were injected i.p. with escalating doses of morphine (20–100 mg/kg) for three days, and then physical signs of morphine withdrawal were monitored during a 30-min period after the injection of 1 mg/kg naloxone (an opioid receptor antagonist). No difference in the morphine withdrawal symptoms was observed between the two genotypes (jumping: WT, 58.0 ± 11.9, KO, 52.4 ± 4.9, $P = 0.673$; paw tremor: WT, 140 ± 25.8, KO, 158 ± 39.5, $P = 0.724$, $n = 5$ each).

Addictive Responses to Morphine and Cocaine in Tam$^{-/-}$ KO Mice. We next investigated the addictive effects of repeated administration of morphine and cocaine to Tam$^{-/-}$ KO and WT mice. Morphine can establish preference for an environment associated with repeated morphine exposure. This conditioned place preference (CPP) serves as a model of adaptive responses to repeated morphine administration (21). Mice were conditioned with repeated morphine administration in one of two chambers that differed visually and texturally. Before conditioning, mice visited two chambers with no difference (Fig. 4A). After conditioning with morphine for 3 days, the development of CPP of Tam$^{-/-}$ KO mice was significantly reduced compared with that of WT mice at 3 mg/kg morphine [$P = 0.036$, $n = 11$ (WT) and 12 (KO)]. A higher dose of morphine (5 mg/kg) also tended to reduce the CPP of Tam$^{-/-}$ KO mice, although the difference

Fig. 4. Morphine-induced CPP and cocaine-induced locomotor sensitization. (*A*) CPP was measured before and after conditioning with s.c. injection of the indicated doses of morphine for 3 days. The time difference of CPP was calculated by subtracting the time mice spent in the saline-paired side from the time they spent in the morphine-paired side (*, $P = 0.036$, $n = 8$–12). (*B*) Immediately after the injection of saline or cocaine, locomotor activity was counted for a 10-min period (*, $P < 0.05$, $n = 15$ each).

between the two genotypes was not statistically significant [$P = 0.322$, $n = 8$ (WT) and 9 (KO)] (Fig. 4*A*).

Repeated administration of cocaine induces a progressive increase in locomotor activity, called locomotor sensitization (22). We addressed whether tamalin deficiency would affect locomotor sensitization by daily administering cocaine to mice (Fig. 4*B*). Mice were habituated to the open field for 3 days, and their locomotor activity was measured immediately after injection of saline on days 4 and 5 and after injection of 5 mg/kg cocaine from day 6 to day 10. No genotypic difference in locomotor activity was observed after saline administration (Fig. 4*B*). Tam$^{-/-}$ KO mice showed significantly less locomotor activity on the first ($P = 0.039$, $n = 15$ each) and second ($P = 0.033$) days of cocaine administration. This reduction continued on the third to the fifth day of cocaine administration, although the differences on the third to fifth days were not statistically

significant (Fig. 4*B*). The results demonstrate that tamalin deficiency results in reduced responses to chronic exposure to both morphine and cocaine.

To address the behavioral selectivity involving the neural plasticity of tamalin deficiency, we examined whether learning and memory deficits might accompany tamalin deficiency. The radial maze test (Fig. 5*A*) and contextual and cued fear conditioning test (Fig. 5 *B*–*D*) were conducted to examine genotypic distinctions in learning and memory (12). No genotypic differences were observed in the number of revisits to the arms in the radial maze test (for genotype, $P = 0.633$, $n = 20$ each) (Fig. 5*A*). Also, no genotypic differences in fear conditioning or in contextual and cued conditioning fear memories were observed between the two genotypes (for genotype, fear conditioning, $P = 0.903$; contextual fear memory, $P = 0.193$; cued fear memory, $P = 0.568$, $n = 18$ each) (Fig. 5 *B*–*D*). These results indicate that tamalin deficiency selectively impairs the adaptive neural plasticity involved in reinforcement and addiction to drugs of abuse.

Extracellular Dopamine (DA) and Glutamate Levels in the NAc of Tam$^{-/-}$ KO Mice after Morphine Administration. The acute administration of morphine rapidly increases extracellular levels of DA in the NAc (23, 24). We performed *in vivo* microdialysis analysis to address whether tamalin deficiency would influence extracellular DA and glutamate levels in the NAc after morphine administration. Samples were collected from the NAc of conscious, freely moving mice, and extracellular levels of DA and glutamate were assessed by HPLC before and after injection of morphine (2.5 mg/kg, s.c.). Basal levels of DA [WT, 0.60 ± 0.122 nM; KO, 0.59 ± 0.084 nM; $P = 0.933$; $n = 4$ (WT) and 6 (KO)] and glutamate [WT, 120.4 ± 8.9 nM; KO, 114.7 ± 6.8 nM; $P = 0.628$; $n = 3$ (WT) and 4 (KO)] before morphine administration were comparable between WT and Tam$^{-/-}$ KO mice. Morphine administration rapidly increased the extracellular DA levels in both genotypes, but no significant difference was observed between the two genotypes [for genotype, $P = 0.881$, $n = 4$ (WT) and 6 (KO)] (Fig. 6). Morphine administration had no effect on glutamate release in the NAc of either WT or Tam$^{-/-}$ KO mice. Thus, tamalin deficiency has no direct effect on the release of either of these neurotransmitters in the NAc.

Discussion

Tamalin is an evolutionarily highly conserved scaffold protein and possesses a PDZ domain, a leucine zipper region, and a PDZ-binding motif (7). The multiple protein domains of tamalin interact with many neuronal proteins involved in synaptic transmission and neuronal development (5–9). Thus, we did not expect that Tam$^{-/-}$ KO mice would show no obvious behavioral

Fig. 5. Radial maze test (*A*) and contextual and cued fear conditioning (*B*–*D*). (*A*) In the eight-arm radial maze test, the number of revisits to the arms to obtain all eight pellets in each arm is presented for each trial. Mice went through 1 trial per day from trial 1 to trial 8 and two trials per day from trial 9 to trial 22. (*B*) Mice freely moved in a sound-attenuated chamber for the first 2 min. The conditioned stimulus (CS) was presented for 30 sec, followed by the unconditioned stimulus (US) for 2 sec. Two more CS–US pairings were presented with a 2-min interstimulus interval. Freezing was calculated every 1 min for 8 min, and percentages of freezing are presented from the beginning of analysis. (*C*) Contextual fear responses were tested every 1 min for 5 min 1 day after the above conditioning. (*D*) Cued fear responses with altered context were tested every 1 min for 6 min 1 day after conditioning of the above mice by using a triangular box, which was located in a different room. CS was presented for 3 min from 3 min after placing mice in the different environment.
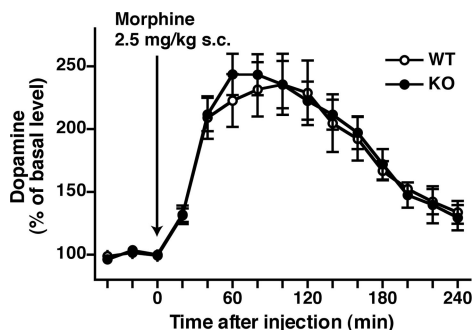
Fig. 6. *In vivo* microdialysis analysis of DA after morphine administration. After collection of 3 baseline fractions, morphine (2.5 mg/kg, s.c.) was administered, and 12 fractions were collected, 1 every 20 min. Data are normalized to percentage changes by the average value of 3 baseline fractions.

abnormality under ordinary conditions, or any appreciable developmental or architectural changes in their brain. Cytohesin-binding protein (CBP) is a closely related protein that possesses a PDZ domain and a leucine zipper domain (5). However, CBP lacks all other protein motifs characteristic of tamalin and is not expressed in the brain (5). It is thus unlikely that this lack of obvious phenotypic abnormalities in Tam$^{-/-}$ KO mice is due to redundancy of the tamalin-related gene family. This investigation was thus extended further to the analysis of more defined and enforcing behavioral changes, and the results indicated that tamalin deficiency caused a significant reduction in the sensitivity to morphine in the acute response and to morphine and cocaine in adaptive responses.

The important neural network for actions of morphine and cocaine is the mesolimbic DA system, which originates in the ventral tegmental area (VTA) and targets the NAc (15–18). Morphine primarily acts on μ-opioid receptors and suppresses GABAergic interneurons in the VTA. This suppression disinhibits DA neurons in the VTA and, in turn, leads to an increased level of DA in the NAc (23, 24). Also, cocaine blocks the activity of DA transporters, which results in an increased DA level in the NAc (24). DA thus plays a central role in both morphine and cocaine actions. In addition, the convergent interaction of DA and glutamate in the NAc is important for controlling the cellular and behavioral responses to drugs of abuse (15–18). Our *in vivo* microdialysis experiment confirmed a marked and rapid morphine-induced increase in extracellular DA without any change in extracellular glutamate in the NAc. However, neither basal and induced levels of DA, nor those of glutamate, were different between WT and Tam$^{-/-}$ KO mice. These findings suggest that the altered responses to morphine and cocaine in Tam$^{-/-}$ KO mice result from impaired scaffold function and/or intracellular signaling of tamalin rather than dysregulation of synaptic neurotransmitters.

Recently, several scaffold proteins have been implicated in both cellular and behavioral responses to morphine and cocaine. PSD-95 is markedly down-regulated in the striatum, and long-term potentiation (LTP) is enhanced at the frontocortical-NAc glutamatergic synapses after chronic cocaine treatment (25). Targeted deletion of PSD-95 persistently enhances LTP and augments the acute locomotor-stimulating effects of cocaine (25). Deletion of Homer2 augments extracellular glutamate in the NAc and alters regulation of glutamate by mGluR1 and cystine/glutamate exchange (26). The Homer2 knockout mice show cocaine-sensitized phenotypes including enhanced cocaine-induced locomotion and CPP (26). Deletion of β-arrestin-2 impairs the acute locomotor stimulant effect of morphine but conversely enhances adaptive responses to morphine such as morphine antinociceptive tolerance and CPP (27,

28). The behavioral alterations in acute and chronic responses to morphine and cocaine are thus different between Tam$^{-/-}$ KO mice and those reported for the other scaffold proteins. Tamalin is involved in protein assembly of key synaptic receptors and multiple protein-trafficking and signaling proteins (5–9). For example, tamalin-associated cytohesins control the activity of the ARF family (29). The ARF family is involved in endocytosis, recycling of target proteins, actin reorganization, and intracellular signaling (30–32). Furthermore, group 1 mGluRs have been shown to be important for both acute and chronic responses to morphine and cocaine (18). Tamalin not only interacts with group 1 mGluRs but also forms a multimolecular protein assembly comprising c-Src protein kinase and SHP2 protein phosphatase (8). Tamalin also mediates Syk kinase signaling in an immunoreceptor tyrosine-based activation motif-based fashion (8). Although the mechanisms underlying tamalin-mediated behavioral responses need further investigation, the distinctive behavioral alterations of Tam$^{-/-}$ KO mice provide a clue to study novel spatiotemporal molecular assembly and signal transduction in tamalin-mediated neural and behavioral plasticity *in vivo*.

Materials and Methods

Generation of Tamalin Mutant Mice. A 129/SvJ mouse DNA library (Stratagene, La Jolla, CA) was used for isolation of genomic fragments containing the tamalin gene. Electroporation of the vector DNA into CCE ES cells, isolation of recombinant clones, and generation of chimeric mice were carried out as described in ref. 33. Another targeting vector was constructed from a C57BL/6 BAC genomic clone (BACPAC Resources, Oakland, CA). The basic design of this targeting vector was the same as the one described above. The targeting vector was electroporated into TT2 ES cells (34). One and two independent germ-line chimeric mice were obtained from the 129/Sv allele and C57BL/6 allele, respectively. Mouse lines harboring the mutation in the 129/Sv allele and C57BL/6 allele (CDB0420K) were each crossed with *EIIa-Cre* transgenic mice on a C57BL/6 genetic background (a gift from U. Rudolph, University of Zurich, Zurich, Switzerland). All animals used in this investigation were handled according to guidelines of Kyoto University Faculty of Medicine and the Animal Research Committee of the Osaka Bioscience Institute.

Immunohistochemistry and Immunoblotting. Immunohistochemistry of parasagittal sections (20 μm) of the mouse adult brain was performed as described previously (35). For immunoblotting (8), the brain was quickly removed and sectioned on a brain matrix (Muromachi, Tokyo, Japan) at a thickness of 1 mm. The striatum was isolated from the slices on ice. Rabbit anti-mGluR2 (1:1,000), rabbit anti-GABA$_{B2}$ (1:300), and goat anti-cytohesin-2 (1:200) were obtained from Upstate Biotechnology, Chemicon, and Santa Cruz Biotechnology, respectively. Other antibodies were obtained as described previously (5, 7, 8).

Behavioral Analysis. Heterozygous tamalin mutant mice were backcrossed to the C57BL/6J background for at least seven generations. All experimental mice were generated through mating of heterozygous tamalin mutant mice. For all behavioral studies of morphine and cocaine treatment, 10- to 14-week-old male Tam$^{-/-}$ KO mice and their male WT littermates were used. Mice were used only once for each experiment, and a new group of mice was used for each dose and drug tested. Morphine hydrochloride and cocaine hydrochloride (both from Shionogi, Osaka, Japan) were used for behavioral analysis. A comprehensive physical and behavioral test battery and CPP were performed as described previously (12, 13, 36). Locomotor activity was measured with an infrared activity monitor (27 × 27 × 20 cm; Med Associates, Georgia, VT). The hot-plate and tail-flick tests were performed as described previously (37).

Baseline responses were determined for each mouse before morphine injection. Cutoff times of the hot-plate and tail-flick tests were 30 sec and 10 sec, respectively, to minimize tissue damage. The antinociceptive response was calculated as a percentage of maximal possible effect (%MPE), where %MPE = $100\% \times$ (drug response time − basal response time) / (cutoff time − basal response time). For morphine physical dependence and withdrawal analysis, mice were injected i.p. with escalating doses of morphine (20, 40, 60, 80, 100, 100, and 100 mg/kg) every 8 h for 3 days. Two hours after the last morphine injection, naloxone (1 mg/kg; Sankyo, Tokyo) was administered s.c., and withdrawal behaviors (jumping and paw tremor) were then monitored for 30 min.

The eight-arm radial maze test was conducted as described previously (12). The contextual fear conditioning was performed in a sound-attenuated test chamber ($26 \times 34 \times 29$ cm) as described in ref. 12. A 55-dB white noise and a mild footshock (2 sec, 0.3 mA) were used, respectively, as a conditioned stimulus (CS) and an unconditioned stimulus (US). Cued testing with altered context was conducted after conditioning using a triangular box ($35 \times 35 \times 40$ cm) made of white opaque Plexiglas, which was located in a different room.

***In Vivo* Microdialysis.** *In vivo* microdialysis was performed as described previously (36).

Statistical Analysis. Statistical analysis was conducted by using STATVIEW (SAS Institute, Cary, NC). Data were analyzed by the two-tailed *t* test, two-way ANOVA, or two-way repeated measures ANOVA. Values in graphs are expressed as the mean ± SEM.

1. Grant SG, O'Dell TJ (2001) *Curr Opin Neurobiol* 11:363–368.
2. Reichardt LF (2006) *Philos Trans R Soc London B* 361:1545–1564.
3. Kim E, Sheng M (2004) *Nat Rev Neurosci* 5:771–781.
4. Hall RA, Lefkowitz RJ (2002) *Circ Res* 91:672–680.
5. Kitano J, Kimura K, Yamazaki Y, Soda T, Shigemoto R, Nakajima Y, Nakanishi S (2002) *J Neurosci* 22:1280–1289.
6. Nevrivy DJ, Peterson VJ, Avram D, Ishmael JE, Hansen SG, Dowell P, Hruby DE, Dawson MI, Leid M (2000) *J Biol Chem* 275:16827–16836.
7. Kitano J, Yamazaki Y, Kimura K, Masukado T, Nakajima Y, Nakanishi S (2003) *J Biol Chem* 278:14762–14768.
8. Hirose M, Kitano J, Nakajima Y, Moriyoshi K, Yanagi S, Yamamura H, Muto T, Jingami H, Nakanishi S (2004) *J Biol Chem* 279:32308–32315.
9. Esteban PF, Yoon HY, Becker J, Dorsey SG, Caprari P, Palko ME, Coppola, V, Saragovi HU, Randazzo PA, Tessarollo L (2006) *J Cell Biol* 173:291–299.
10. Holzenberger M, Lenzner C, Leneuve P, Zaoui R, Hamard G, Vaulont S, Bouc YL (2000) *Nucleic Acids Res* 28:E92.
11. Lakso M, Pichel JG, Gorman JR, Sauer B, Okamoto Y, Lee E, Alt FW, Westphal H (1996) *Proc Natl Acad Sci USA* 93:5860–5865.
12. Miyakawa T, Yamada M, Duttaroy A, Wess J (2001) *J Neurosci* 21:5239–5250.
13. Miyakawa T, Leiter LM, Gerber DJ, Gainetdinov RR, Sotnikova TD, Zeng H, Caron MG, Tonegawa S (2003) *Proc Natl Acad Sci USA* 100:8987–8992.
14. Shigemoto R, Mizuno N (2000) in *Handbook of Chemical Neuroanatomy*, eds Otterson OP, Storm-Mathisen J (Elsevier, New York), Vol 18, pp 63–98.
15. Nestler EJ (2001) *Nat Rev Neurosci* 2:119–128.
16. Hyman SE, Malenka RC, Nestler EJ (2006) *Annu Rev Neurosci* 29:565–598.
17. Kalivas PW (2004) *Curr Opin Pharmacol* 4:23–29.
18. Kenny PJ, Markou A (2004) *Trends Pharmacol Sci* 25:265–272.
19. Kieffer BL (1999) *Trends Pharmacol Sci* 20:19–26.
20. Bailey CP, Connor M (2005) *Curr Opin Pharmacol* 5:60–68.
21. Bardo MT, Bevins RA (2000) *Psychopharmacology (Berlin)* 153:31–43.
22. Robinson TE, Berridge KC (2001) *Addiction* 96:103–114.
23. Johnson SW, North RA (1992) *J Neurosci* 12:483–488.
24. Di Chiara G, Imperato A (1988) *Proc Natl Acad Sci USA* 85:5274–5278.
25. Yao WD, Gainetdinov RR, Arbuckle MI, Sotnikova TD, Cyr M, Beaulieu JM, Torres GE, Grant SG, Caron MG (2004) *Neuron* 41:625–638.
26. Szumlinski KK, Dehoff MH, Kang SH, Frys KA, Lominac KD, Klugmann M, Rohrer J, Griffin W, Toda S, Champtiaux NP, *et al.* (2004) *Neuron* 43:401–413.
27. Bohn LM, Gainetdinov RR, Lin FT, Lefkowitz RJ, Caron MG (2000) *Nature* 408:720–723.
28. Bohn LM, Gainetdinov RR, Sotnikova TD, Medvedev IO, Lefkowitz RJ, Dykstra LA, Caron MG (2003) *J Neurosci* 23:10265–10273.
29. Jackson TR, Kearns BG, Theibert AB (2000) *Trends Biochem Sci* 25:489–495.
30. D'Souza-Schorey C, Chavrier P (2006) *Nat Rev Mol Cell Biol* 7:347–358.
31. Hafner M, Schmitz A, Grüne I, Srivatsan SG, Paul B, Kolanus W, Quast T, Kremmer E, Bauer I, Famulok M (2006) *Nature* 444:941–944.
32. Fuss B, Becker T, Zinke I, Hoch M (2006) *Nature* 444:945–948.
33. Masu M, Iwakabe H, Tagawa Y, Miyoshi T, Yamashita M, Fukuda Y, Sasaki, H, Hiroi K, Nakamura Y, Shigemoto R, *et al.* (1995) *Cell* 80:757–765.
34. Yagi T, Tokunaga T, Furuta Y, Nada S, Yoshida M, Tsukada T, Saga Y, Takeda N, Ikawa Y, Aizawa S (1993) *Anal Biochem* 214:70–76.
35. Kitano J, Nishida M, Itsukaichi Y, Minami I, Ogawa M, Hirano T, Mori Y, Nakanishi S (2003) *J Biol Chem* 278:25101–25108.
36. Morishima Y, Miyakawa T, Furuyashiki T, Tanaka Y, Mizuma H, Nakanishi S (2005) *Proc Natl Acad Sci USA* 102:4170–4175.
37. Hikida T, Kitabatake Y, Pastan I, Nakanishi S (2003) *Proc Natl Acad Sci USA* 100:6169–6173.